Earthscope Imaging Science & CIG Seismology Workshop

Introduction to Direct Imaging Methods

Alan Levander
Department of Earth Science
Rice University

Two classes of scattered wave imaging systems

1. *Incoherent imaging systems* which are frequency and amplitude sensitive. Examples are
    1. Photography
    2. Military Sonar
    3. Some deep crustal reflection seismology
    4. Sumatra earthquake source by *Ishii et al. 2005*
2. *Coherent imaging systems* use phase coherence and are therefore sensitive to frequency, amplitude, and phase. Examples are
    1. Medical ultrasound imaging
    2. Military sonar
    3. Exploration seismology

    See *Blackledge, 1989, Quantitative Coherent Imaging: Theory and Applications*

Elements of an imaging algorithm

1. A ***scattering model***
2. A ***wave (de)propagator***
   - *Diffraction and Kirchhoff integrals (Wilson et al., 2005; Levander et al., 2005, 2006)*
   - *One-way* and *two-way finite-difference operators (Claerbout, 1970; 1971; Koslov, 1984)*
   - *Generalized Radon Transforms (Bostock et al., 2001, Rondenay et al., 2001, Schragge et al., 2001)*
   - *Fourier transforms* in space and/or time with phase shifting *(Stolt, 1978; Gazdag, 1978)*
   - *Plane wave decomposition (Poppeliers and Pavlis, 2003)*
3. A focusing criteria known as an ***imaging condition***
4. An estimate of the ***velocity field***
5. Inversion requires iteration using the updated image to generate synthetics and ***repeated backpropagation of data residuals*** *(Tarantola, 1984; Pratt et al., 1998; Pratt, 1999)*

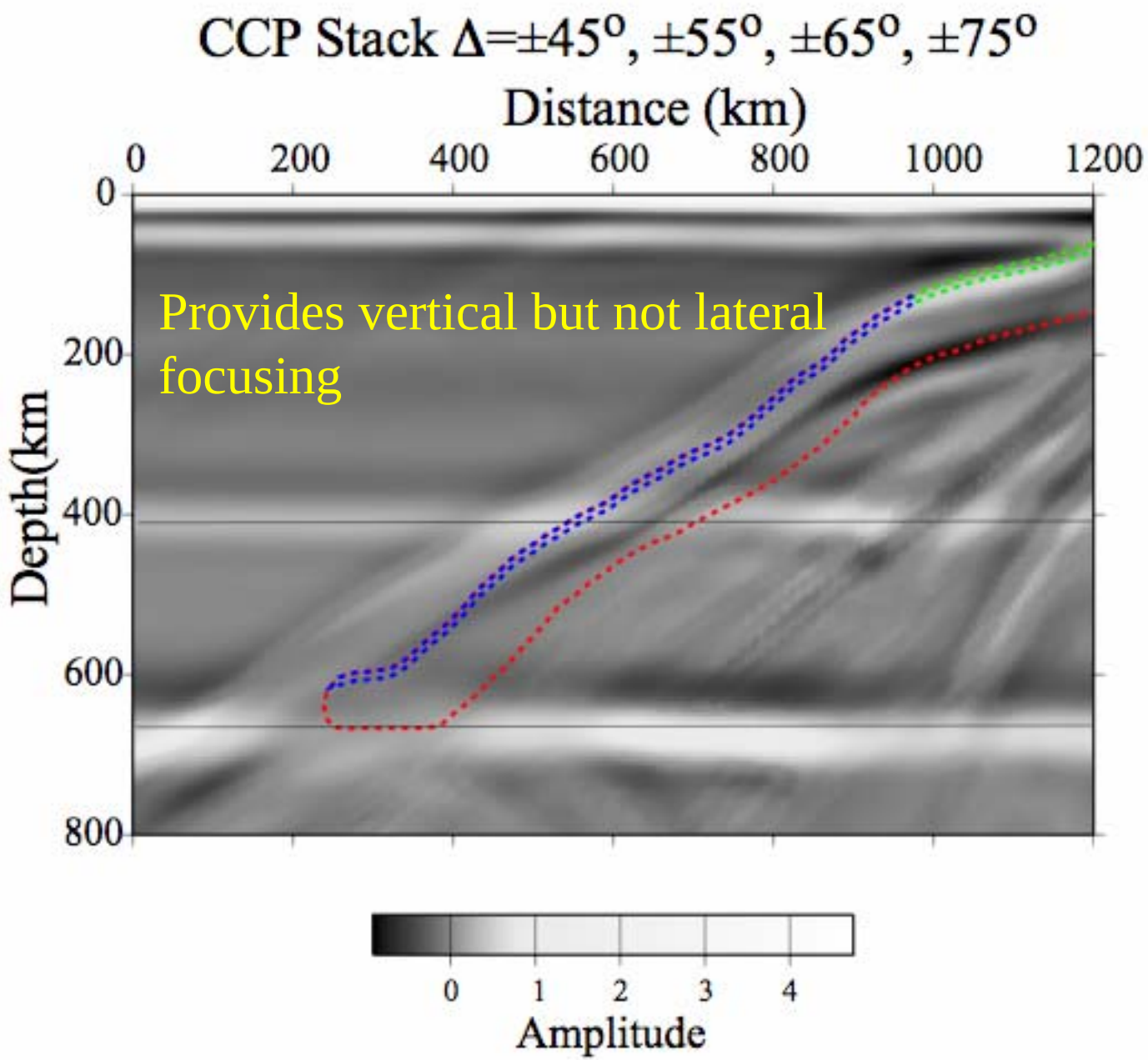
CCP Stack Δ=±45°, ±55°, ±65°, ±75°
Distance (km)
0
200
400
600
800
1000
1200
Depth(km
0
200
400
600
800
Provides vertical but not lateral focusing
0
1
2
3
4
Amplitude

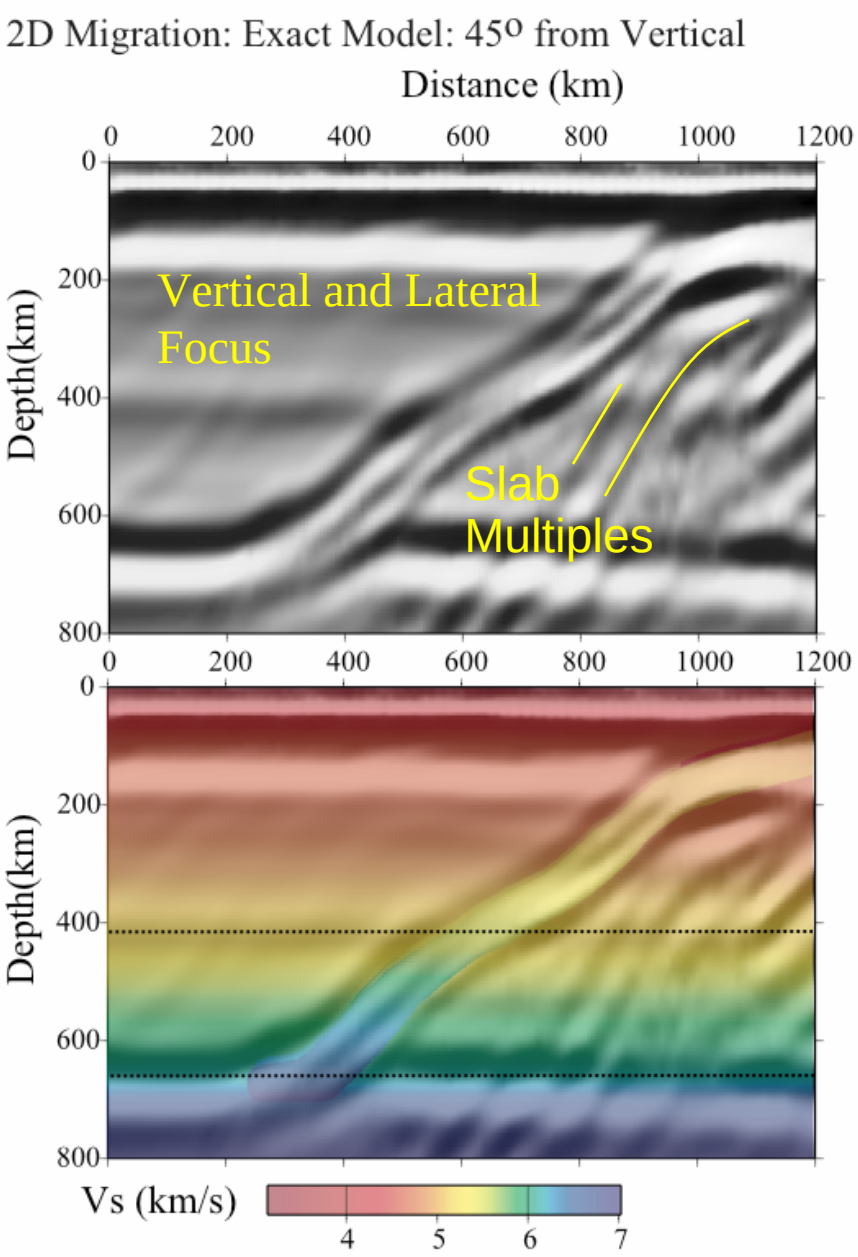

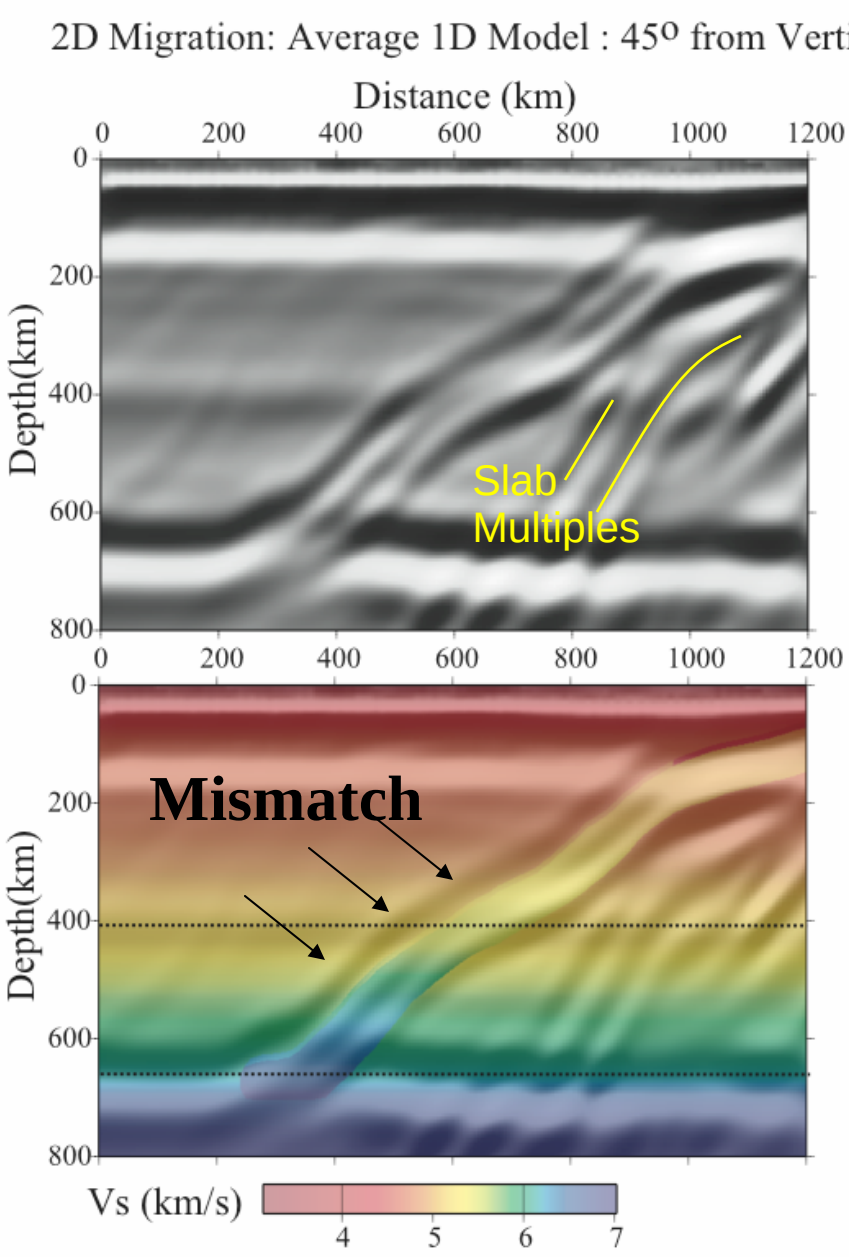

S. Ham, unpublished

Resolution Considerations

- Earthquakes are the only inexpensive energy source able to investigate the mantle
- Coherent Scattered Wave Imaging provides about an order of magnitude better resolution than travel time tomography. For wavelength λ
- $R_{scat} \sim \lambda/2$ versus $R_{tomo} \sim (\lambda L)^{1/2}$
- For a normalized wavelength and path of 100
- $R_{scat} \sim 0.5$ versus $R_{tomo} \sim 10$

Fresnel Zones and other measures of wave sampling

- Fresnel zones
- Banana donuts
- Wavepaths

Are all about the same thing

They are means to estimate the sampling volume for waves of finite-frequency, i.e. not a ray, but a wave.

Flatté et al., *Sound Transmission Through a Fluctuating Ocean*

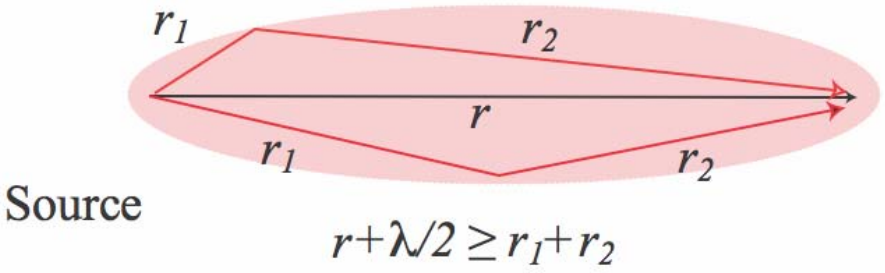

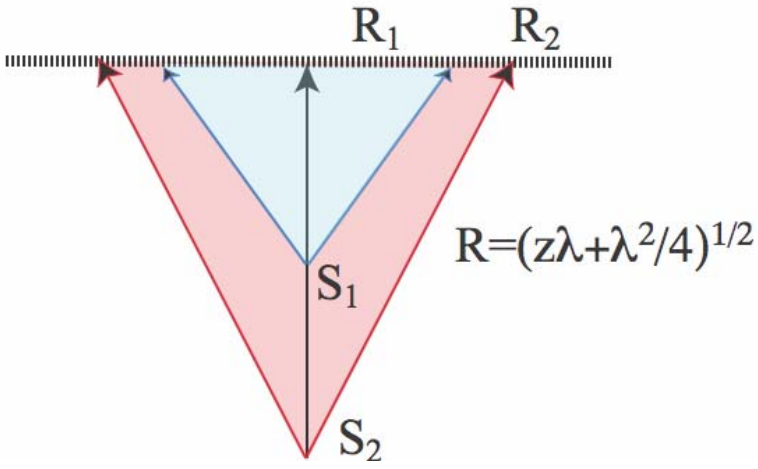

Direct imaging with seismic waves

Converted Wave Imaging from a continuous interface: Receiver Functions (RF)

Images based on this model of 1 D scattering are referred to as common conversion point stacks or

CCP images

These are analogs of seismic reflection images, most sensitive to **Shear velocity perturbations**

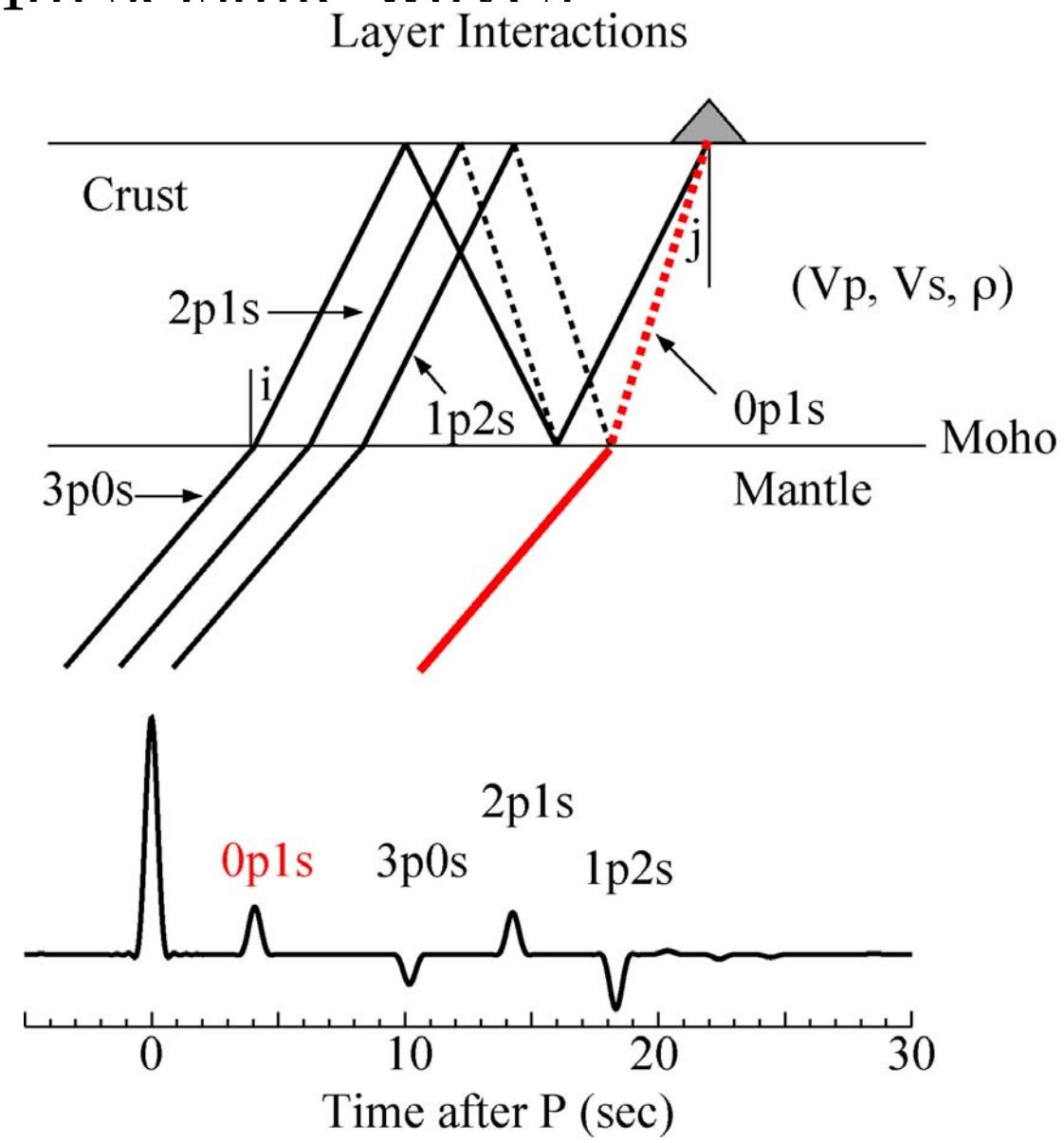

From Niu and James, 2002, EPSL

Scattered wave imaging

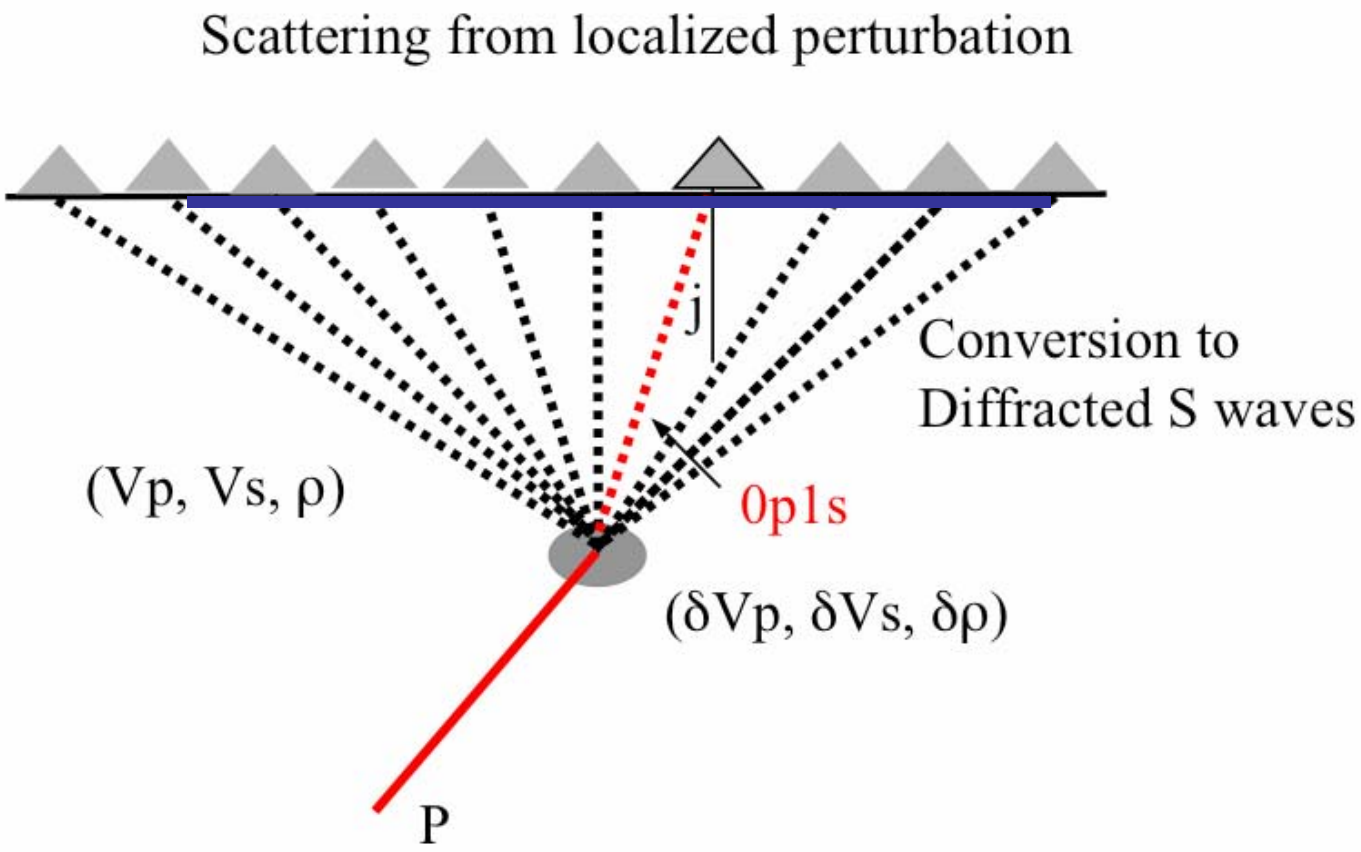

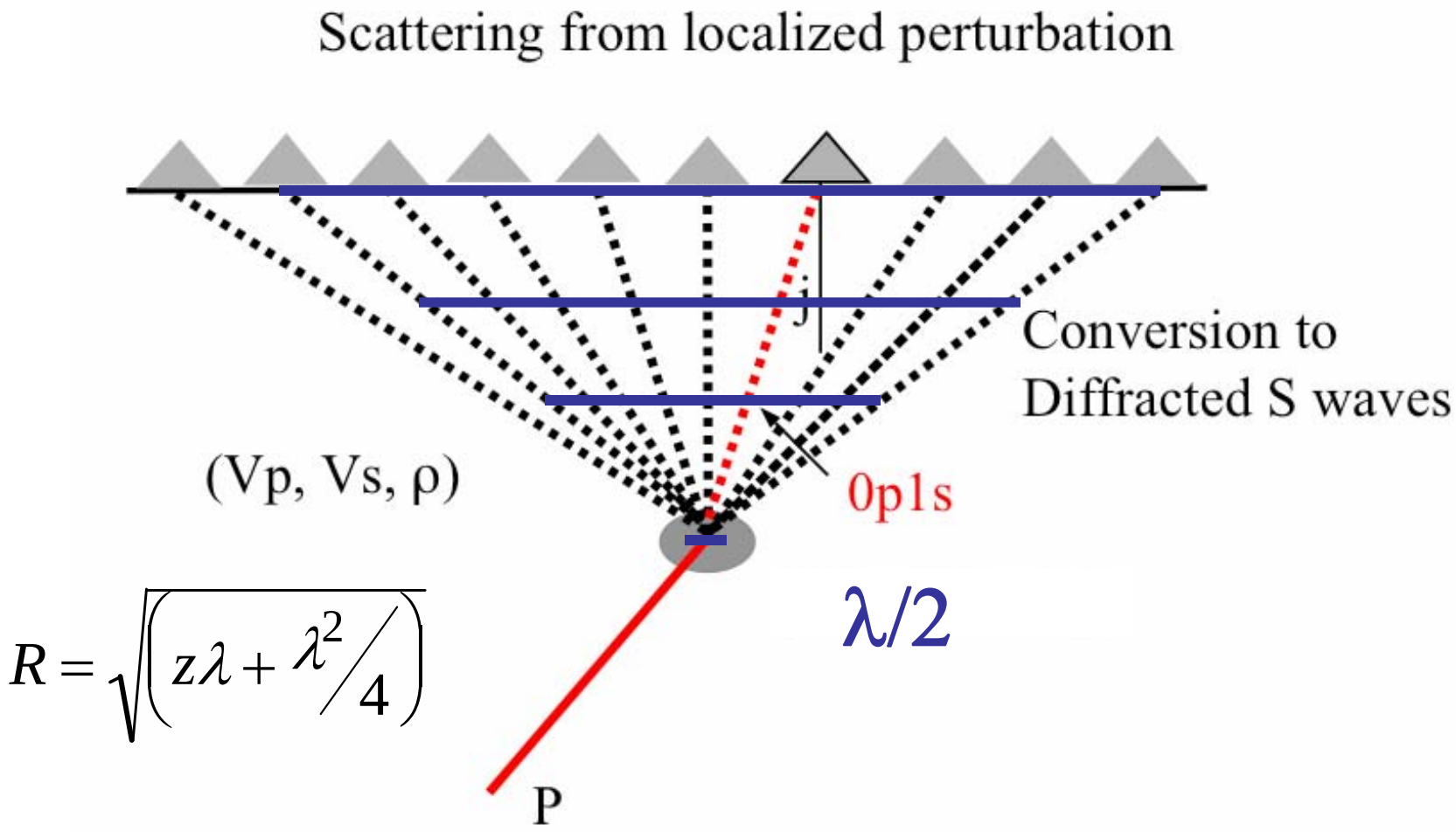

$$R = \sqrt{\left(z\lambda + \lambda^2/4\right)}$$

Scattered wave imaging improves ***lateral*** resolution

It also restores dips

USArray: Bigfoot

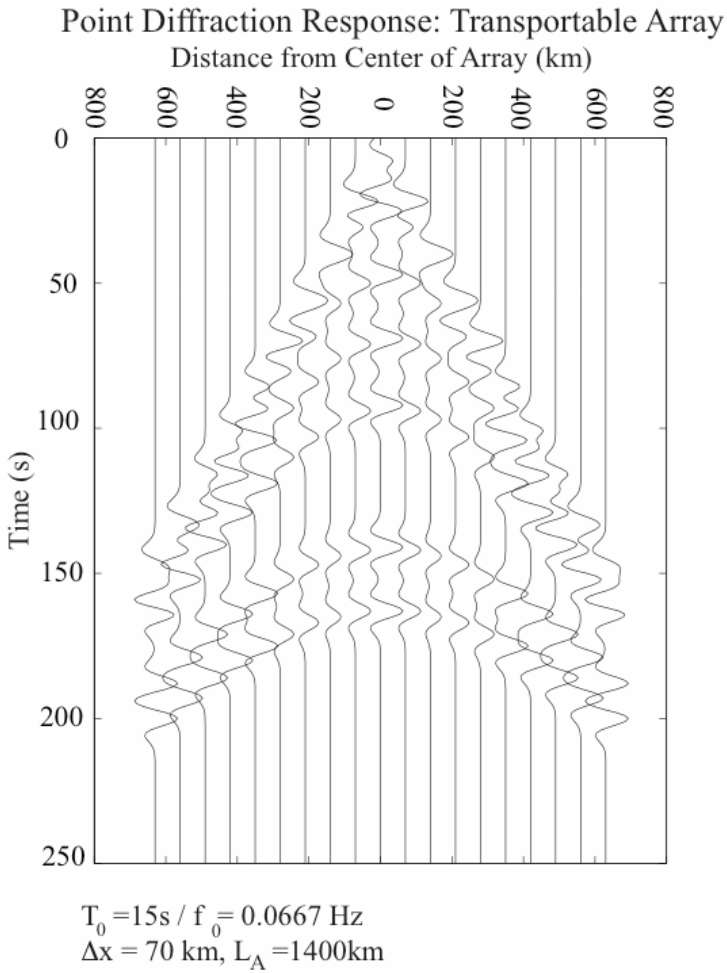

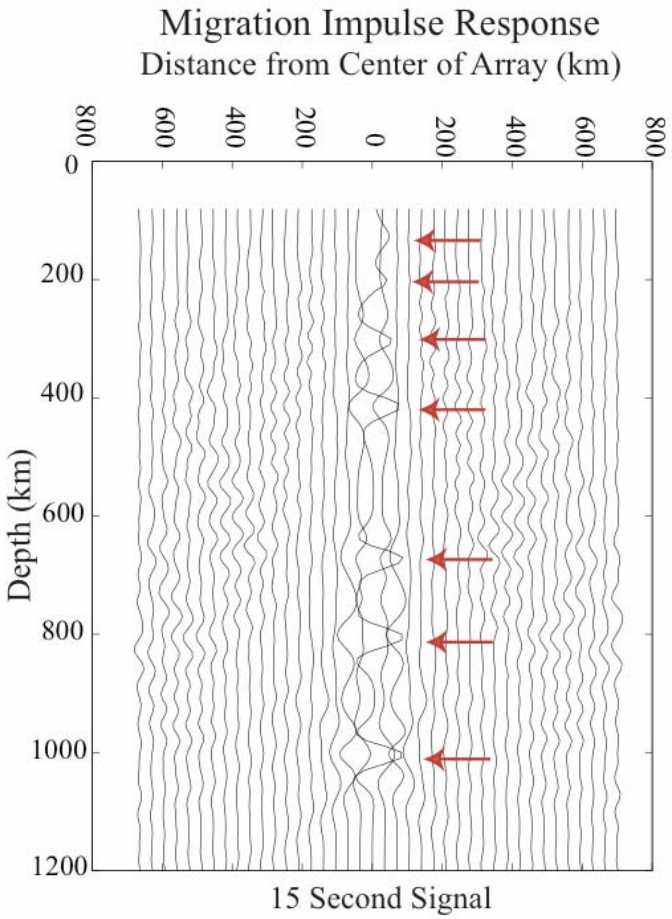

Δx = 70 km, 7s < T < 30s

Imaging Condition

The ***imaging condition*** is given by the time it took the source to arrive at the scatterer plus the time it took the scattered waves to arrive at the receiver. If we have an accurate description of *c(r)* then the waves are focused at the scattering point (attributed to Jon Claerbout)

This is a big if.

For an incident P-wave and a scattered S-wave, and an observation at $\boldsymbol{r_o}$, then the image would focus at point ***r***, when

$$0 = \tau_p(r, r_e) + \tau_s(r_o, r) - t_e(r_o, r_e)$$

Born Scattering

Assume a constant density scalar wave equation with a smoothly varying velocity field *c(x)*

$$\frac{1}{c^2(x)}\frac{\partial^2 U(x,t)}{\partial t^2} - \nabla^2 U(x,t) = f(t)\delta(x - x_s)$$

$$c(x) = \sqrt{\kappa(x)/\rho_o}$$

$$x \in R^n : n = 1,2,3$$

Perturb the velocity field

$$c(x) = c_o(x) + \delta c(x)$$

$$U(x,t) = U_o(x,t) + \delta U(x,t)$$

Born Scattering: Solve for the perturbed field to first order

$$\frac{1}{c^2}\frac{\partial^2 \delta U}{\partial t^2} - \nabla^2 \delta U = \frac{2\delta c}{c^3}\frac{\partial^2 U(x,t)}{\partial t^2}$$

The *total field* consists of two parts, the response to the smooth medium

$$\frac{1}{c^2(x)}\frac{\partial^2 U(x,t)}{\partial t^2} - \nabla^2 U(x,t) = f(t)\delta(x - x_s)$$

Plus the response to the perturbed medium δU

The approximate solution satisfies two inhomogenous wave equations. Note that *energy is not conserved*.
It is the *scattered field* that we use for imaging

- The receiver function:
  - Approximately isolates the SV wave from the P wave
  - Reduces a vector system to a scalar system
  - Allows use of a scalar imaging equation with P and S calculated separately for single scattering: Elastic wave theory:

$$\vec{u}^{P} = \nabla\phi$$

$$\vec{u}^{SV} = \nabla \times \vec{\Psi} : \vec{\Psi} = (0, \psi, 0)$$

The Born Approximation

Perturbing the material property field perturbs the wavefield, let L be the elastic wave operator and m be one of the velocities or density: m= m+δm; m = α, β, ρ; therefore $L \rightarrow L+\delta L$

$$[L+\delta L](u+\delta u) = s(\omega)$$

$$Lu + L\delta u + \delta L u = s(\omega) + O(\delta^2)$$

$$Lu \cong s$$

$$L\delta u \cong -\delta L u$$

$$\delta u = -L^{-1}\delta L u$$

Receiver Function Imaging

$$u = u^P + u^S$$

$$\delta u = \delta u^{PS} + \delta u^{PP} + \delta u^{SS} + \delta u^{SP}$$

$$\delta L = \delta L^{PS} + \delta L^{PP} + \delta L^{SS} + \delta L^{SP}$$

$$\delta u^{PS} = \delta L^{PS} u^P$$

The scattering function for P to S conversion from a heterogeneity
Wu and Aki, 1985, Geophysics

$$U^{PS} = \frac{-V}{4\pi}\frac{\omega^2}{\alpha^2}\left(\frac{\alpha}{\beta}\right)^2 \frac{\exp(-i\omega(t - r/\beta))}{r}$$

$$\times\left[\frac{\delta Z_S}{Z_S}(\sin\vartheta - \frac{\beta}{\alpha}\sin 2\vartheta) - \frac{\delta\beta}{\beta}(\sin\vartheta + \frac{\beta}{\alpha}\sin 2\vartheta)\right]$$

where

$$Z_S = \rho\beta$$

Shear wave impedance

$$\frac{\delta Z_S}{Z_S} = \frac{\delta\rho}{\rho} + \frac{\delta\beta}{\beta}$$

$$-\omega^2 \Leftrightarrow \frac{\partial^2}{\partial t^2}$$

$$\frac{\exp(-i\omega(t - r/\beta))}{r} \Leftrightarrow \frac{\delta(t - r/\beta)}{r}$$

Fourier Transform relations

F6 LevNLC

Signal Detection:

Elastic P to S Scattering from a discrete heterogeneity
Wu and Aki, 1985, Geophysics

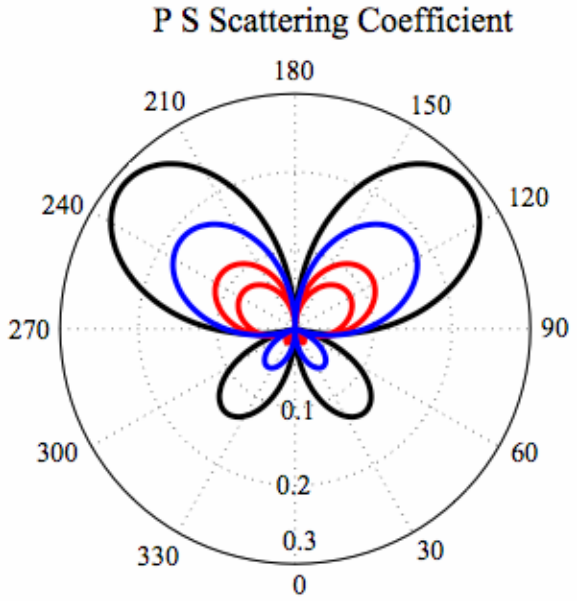

Specular P to S Conversion
Aki and Richards, 1980

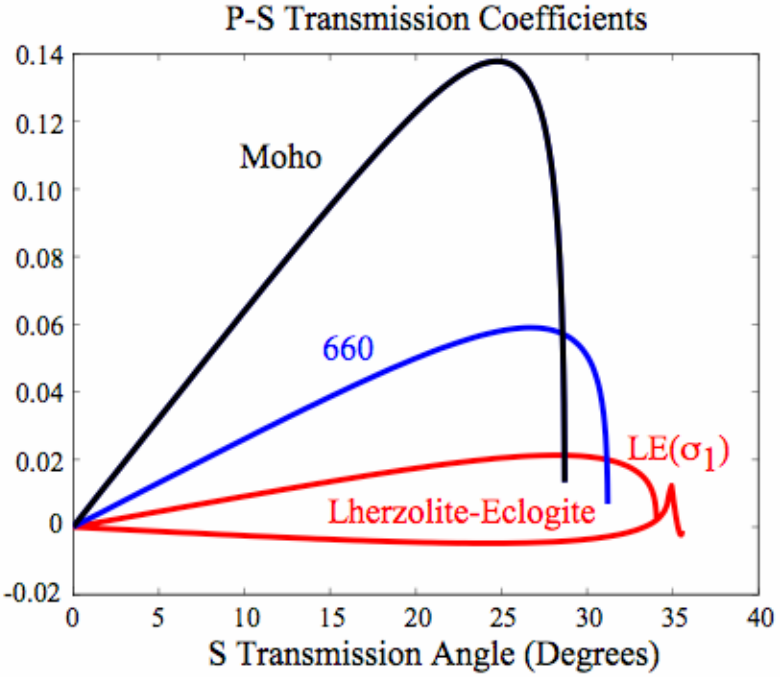

Levander et al., 2006, *Tectonophysics*

The Velocity Field

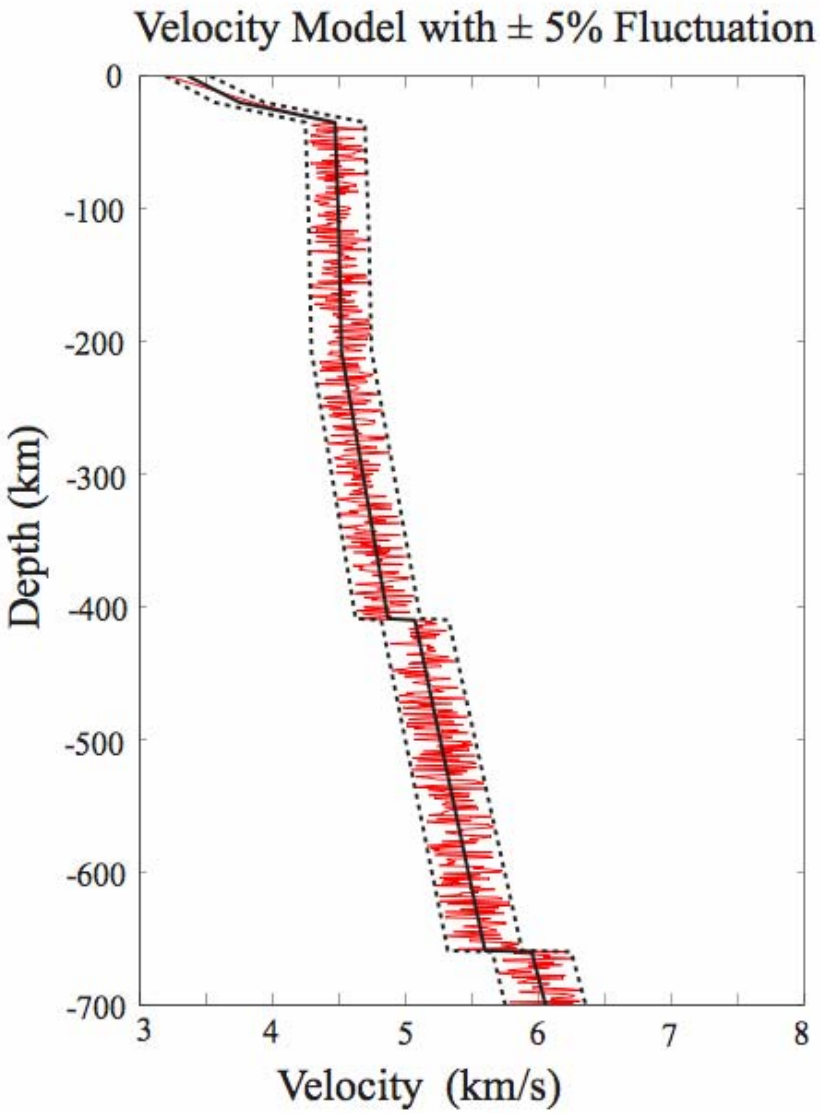

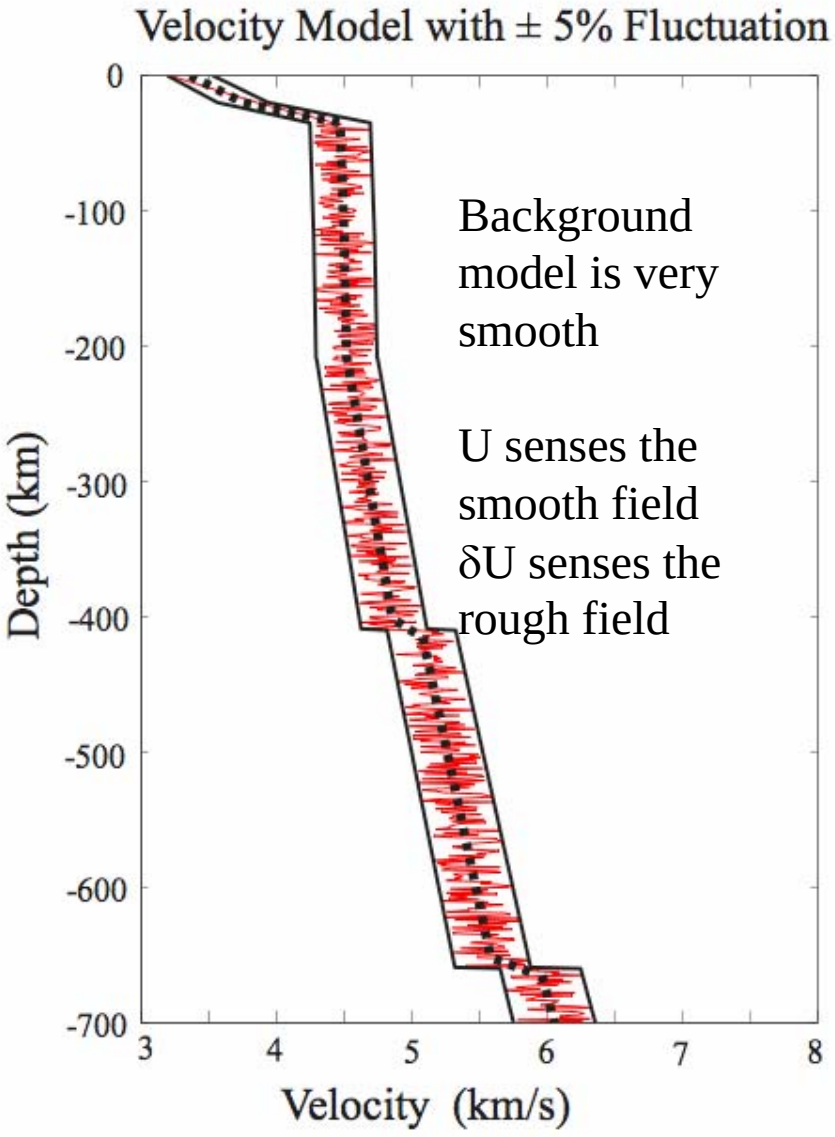

Background model is very smooth

U senses the smooth field
δU senses the rough field

Regional Seismology: PNE Data
Highly heterogeneous models of the CL

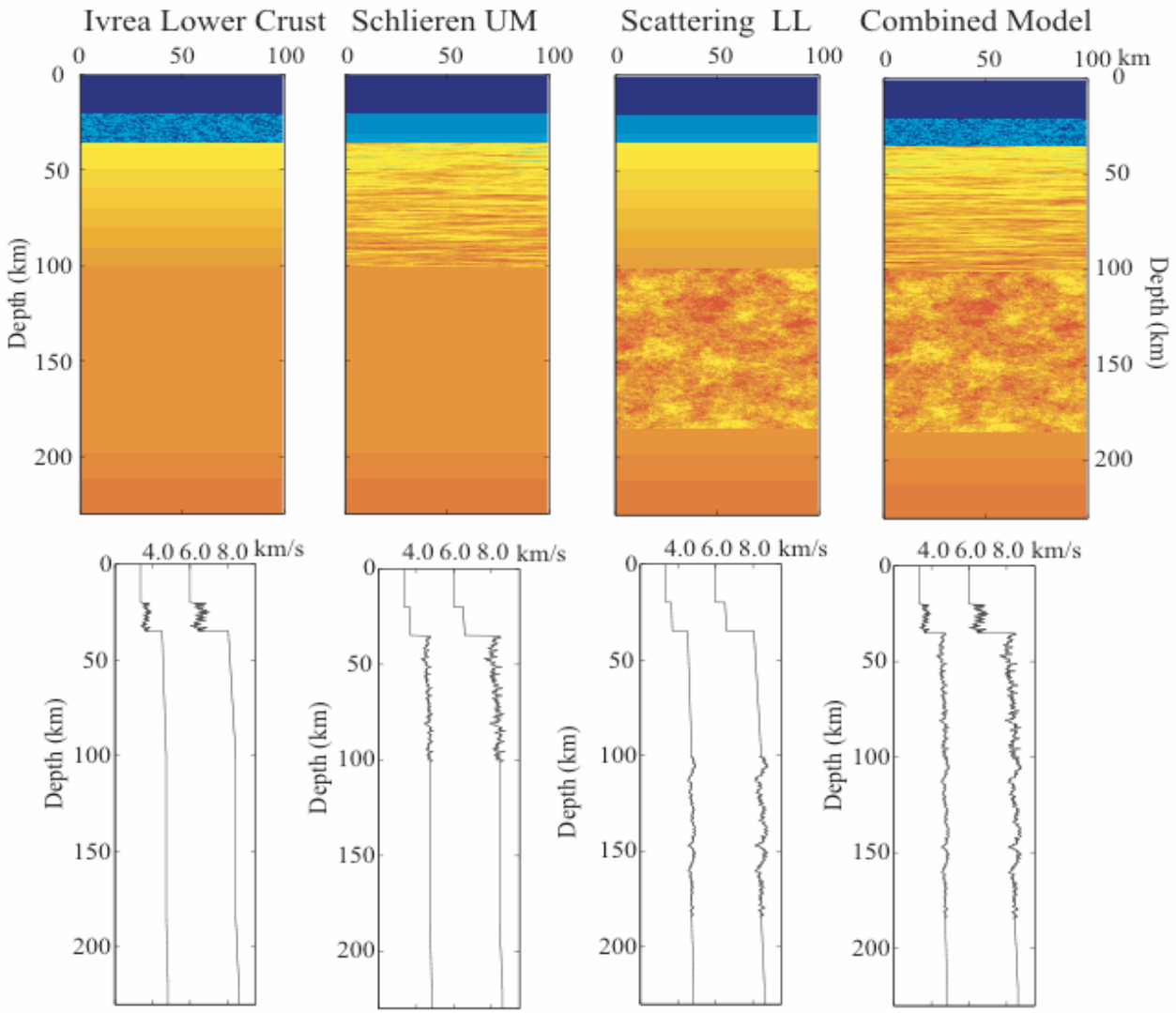

Nielsen et al, 2003, GJI

Definition of an image, from *Scales (1995), Seismic Imaging*

$$I(x) = \square\square PS(x) = \int d\omega \left| F_1(\omega) \frac{u^{Scat}(x,\omega)}{u^{Inc}(x,\omega)} \right|$$

Recall the definition of a receiver function

$$R_F(x_r,t) = \int d\omega \left| F_2(\omega) \frac{u^{SV}(x_r,\omega)}{u^{P}(x_r,\omega)} \right| \exp(-i\omega t)$$

An example of an imaging integral, the Kirchhoff integral using the receiver function

$$I(r) = \square\!\square S(r) = \frac{1}{4\pi^2}\int_{-\infty}^{\infty} d\omega(i\omega)\int_{-L}^{L} dS_0 \exp(-i\omega(t-(\tau_P+\tau_S))R_F(r_0,\omega)\frac{A_S(r,r_0)\cos\theta(r_0)}{A_P(r,r_e)\beta(r_0)}\Bigg|_{t=t_e}$$

1. The scattering model is embedded in the receiver function.
2. The depropagator is the surface integral having the travel times of P and S as a function of surface position.
3. The imaging condition is explicit.
4. The velocity model is implicit in the amplitude and travel time terms.

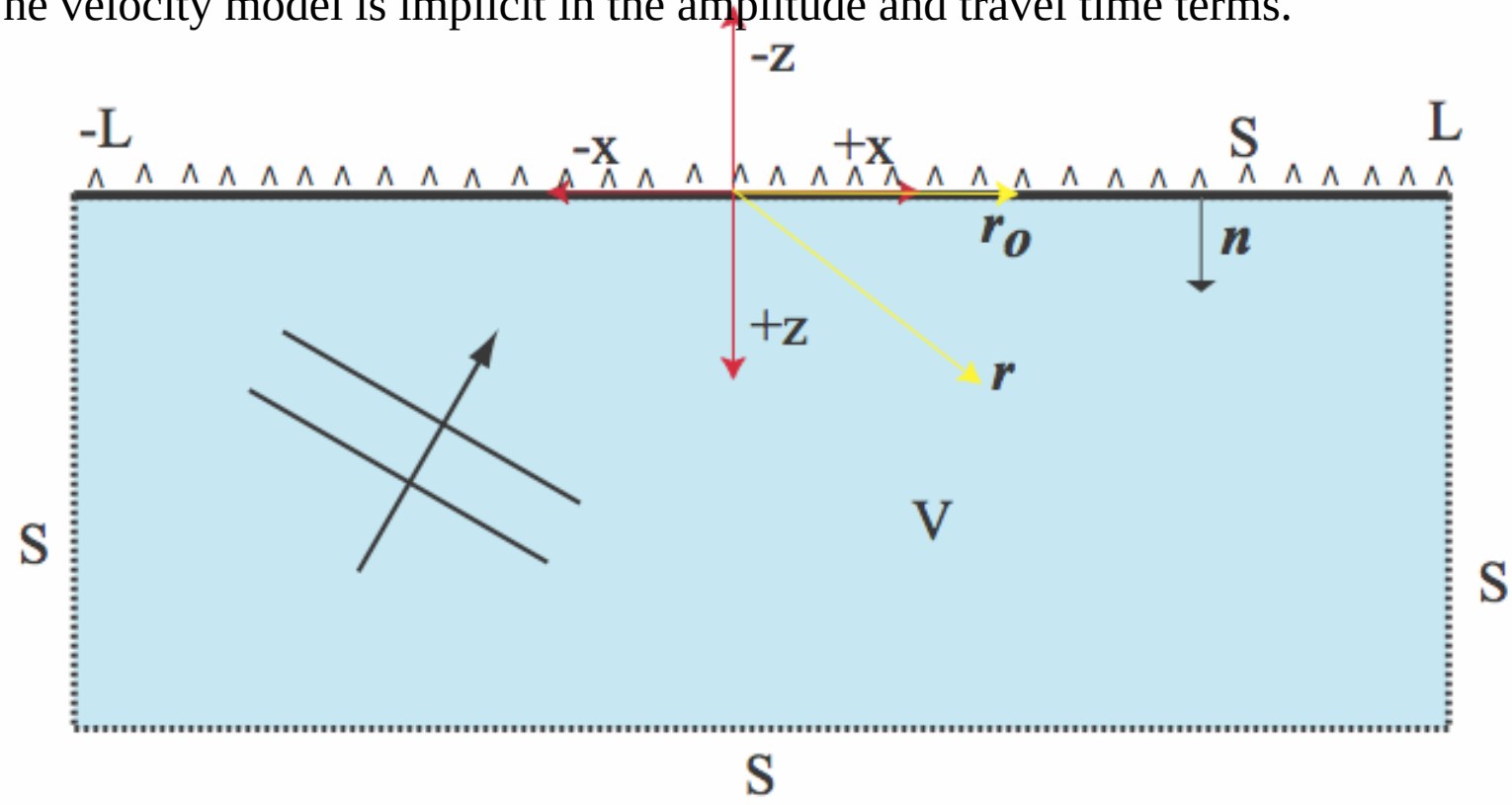

Example:
Kaapvaal
Craton

$\Delta x \sim 35$ km
$A_L \sim 20^o$

9 Eqs

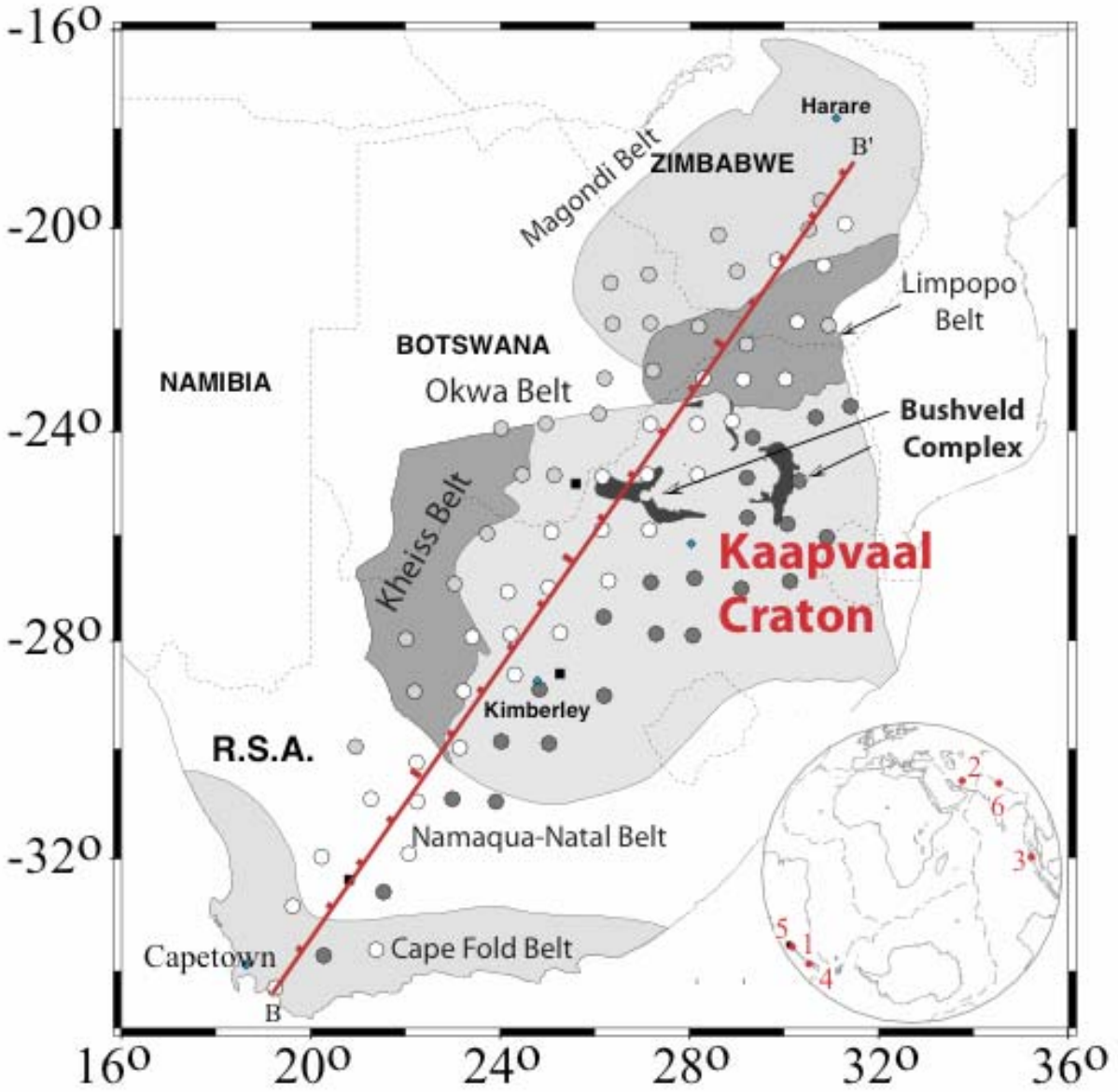

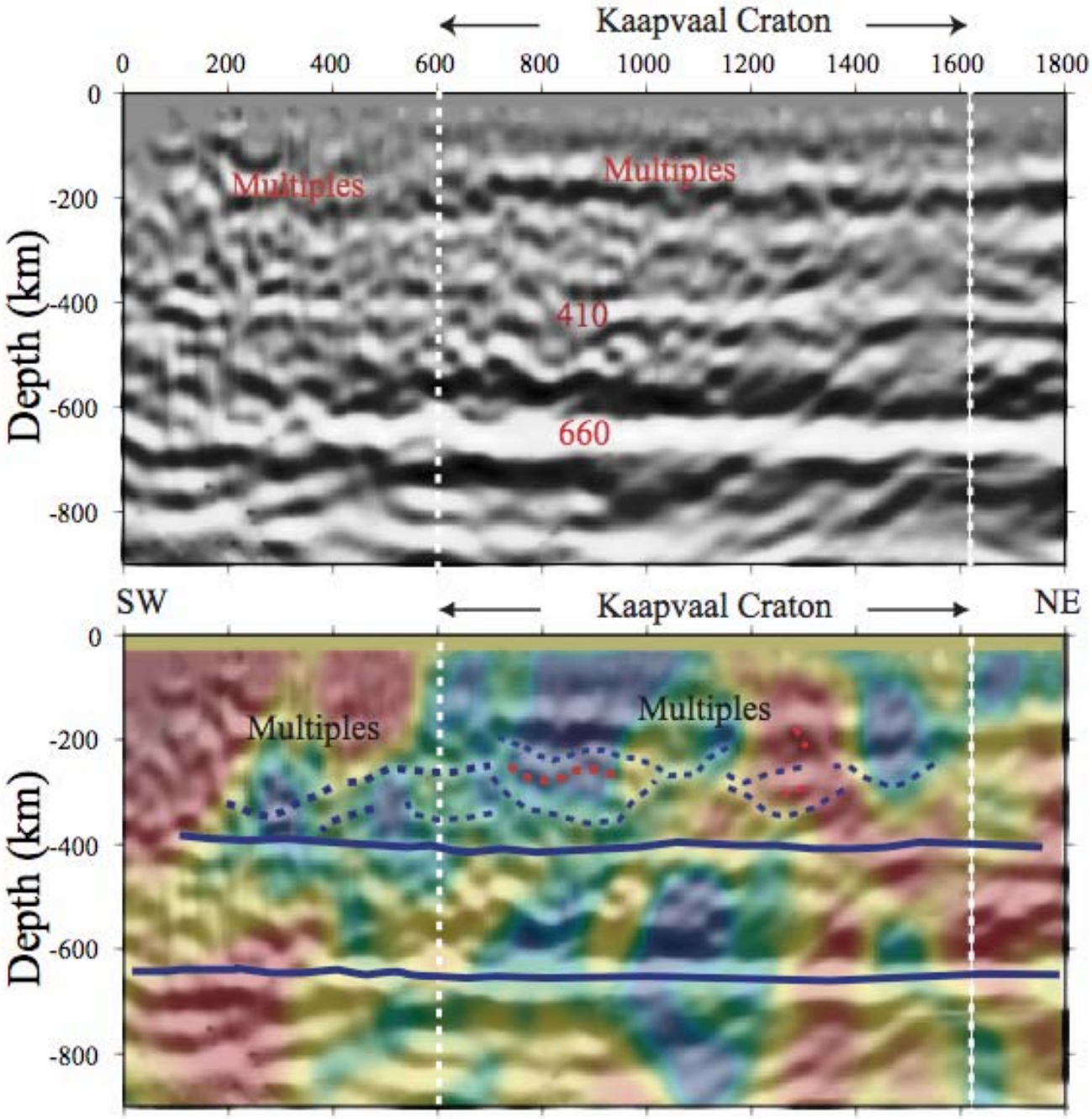

Levander et al., 2005,
AGU Monograph

Hi-Net Geometry: Slab Geometry

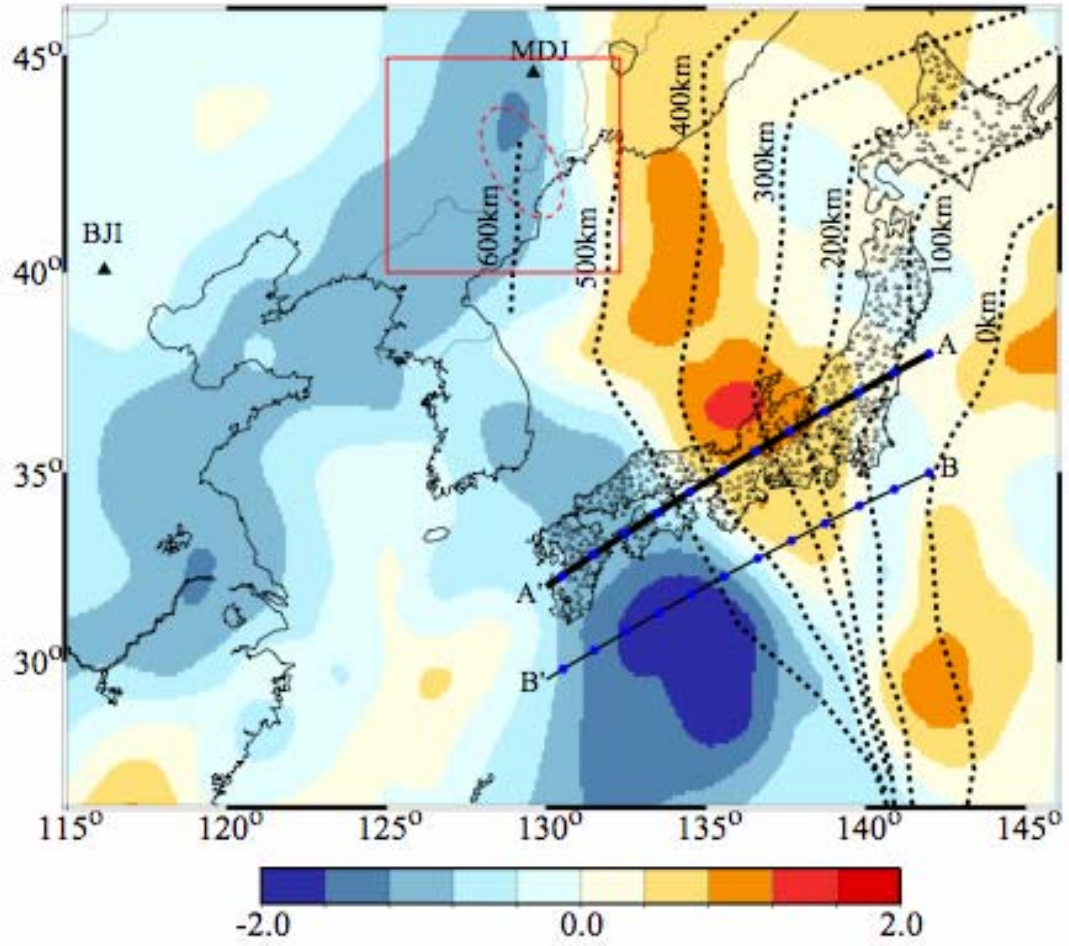

Earthquakes

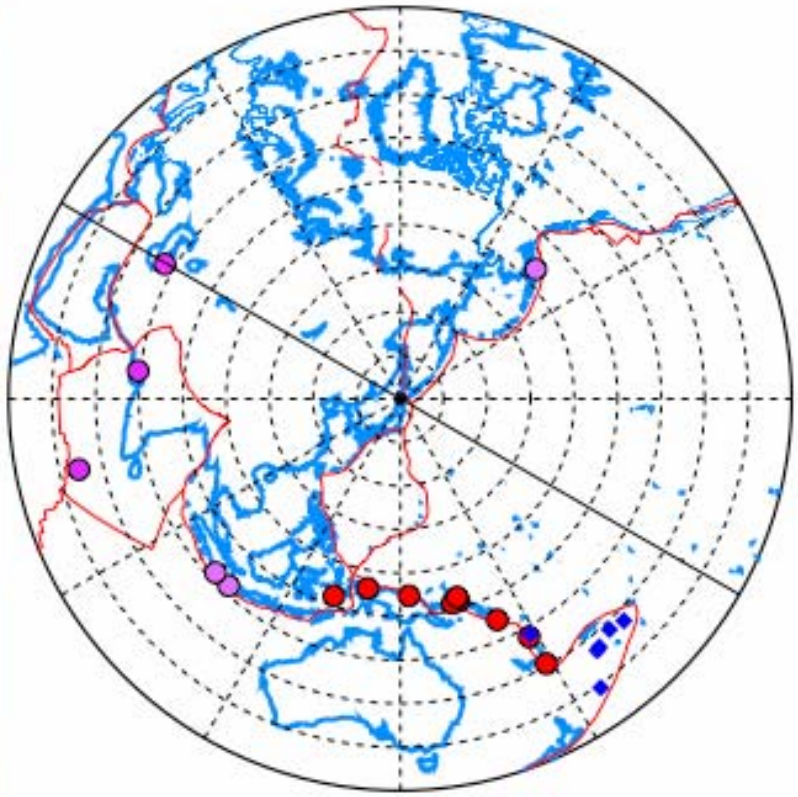

Δx < 10 km / L ~ 1400 km
6 Earthquakes at present

Niu et al., 2005, EPSL

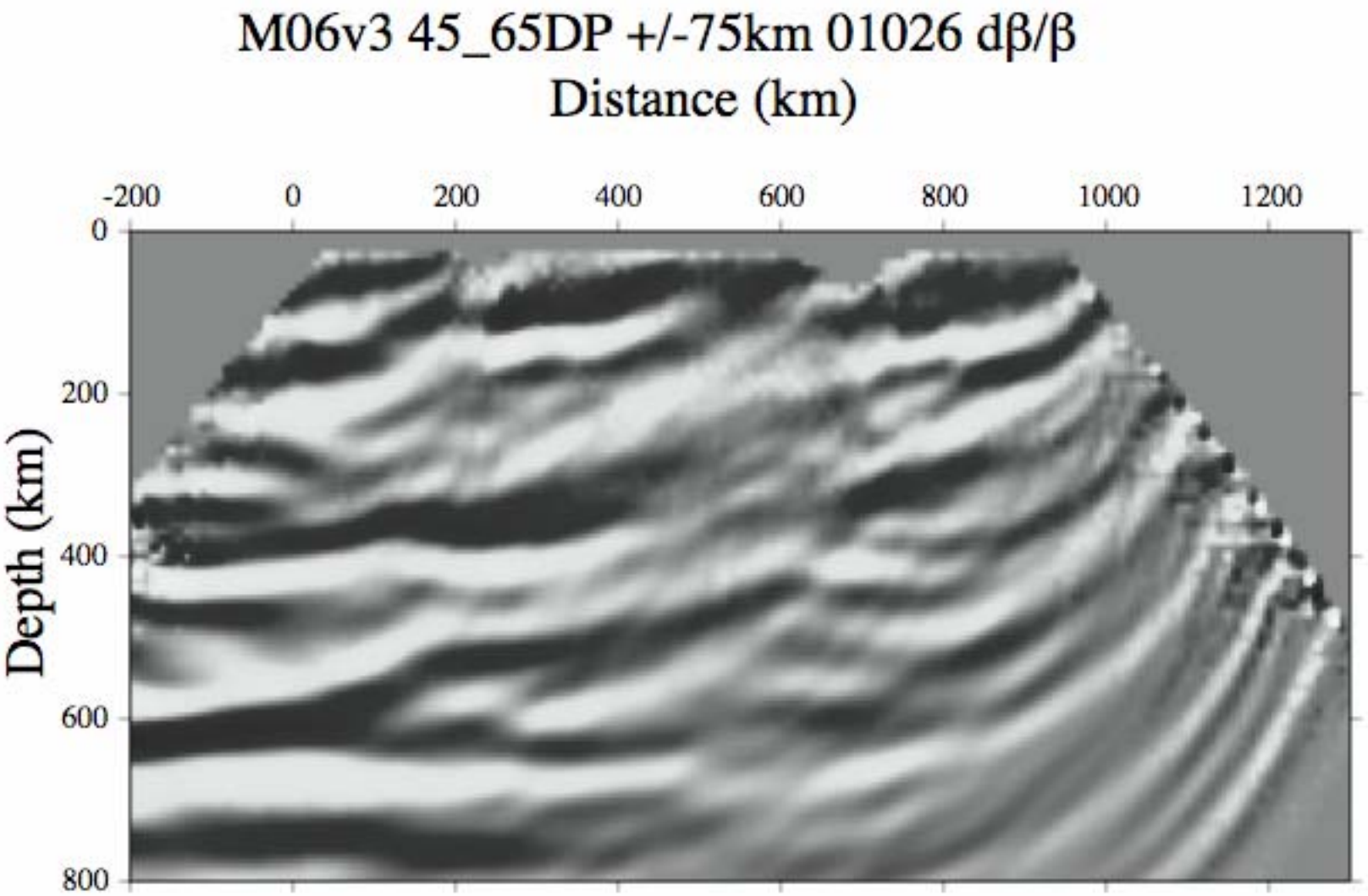

Levander and Niu, 2006, unpublished

P tomography from
Fukao et al, 2001

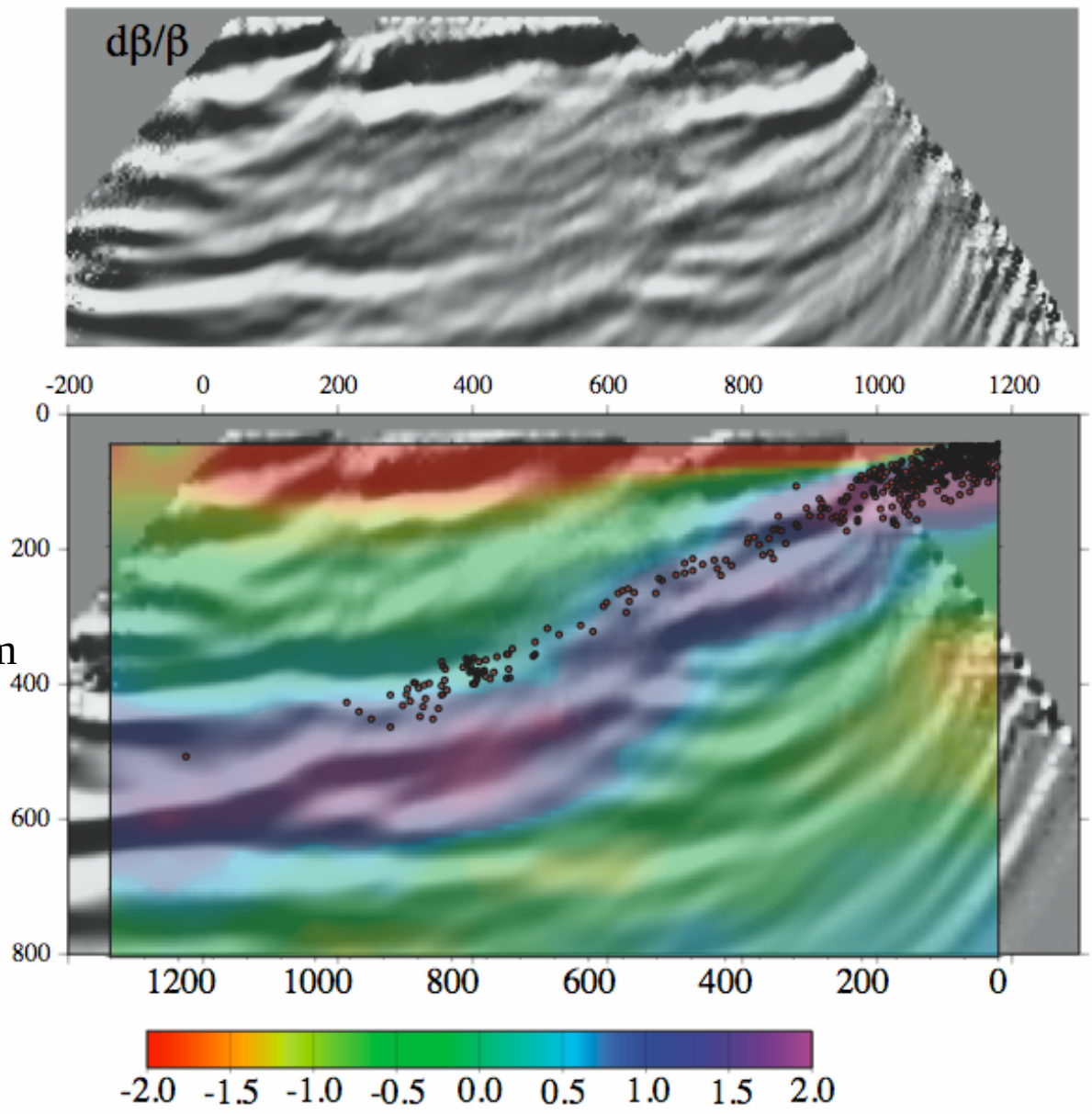

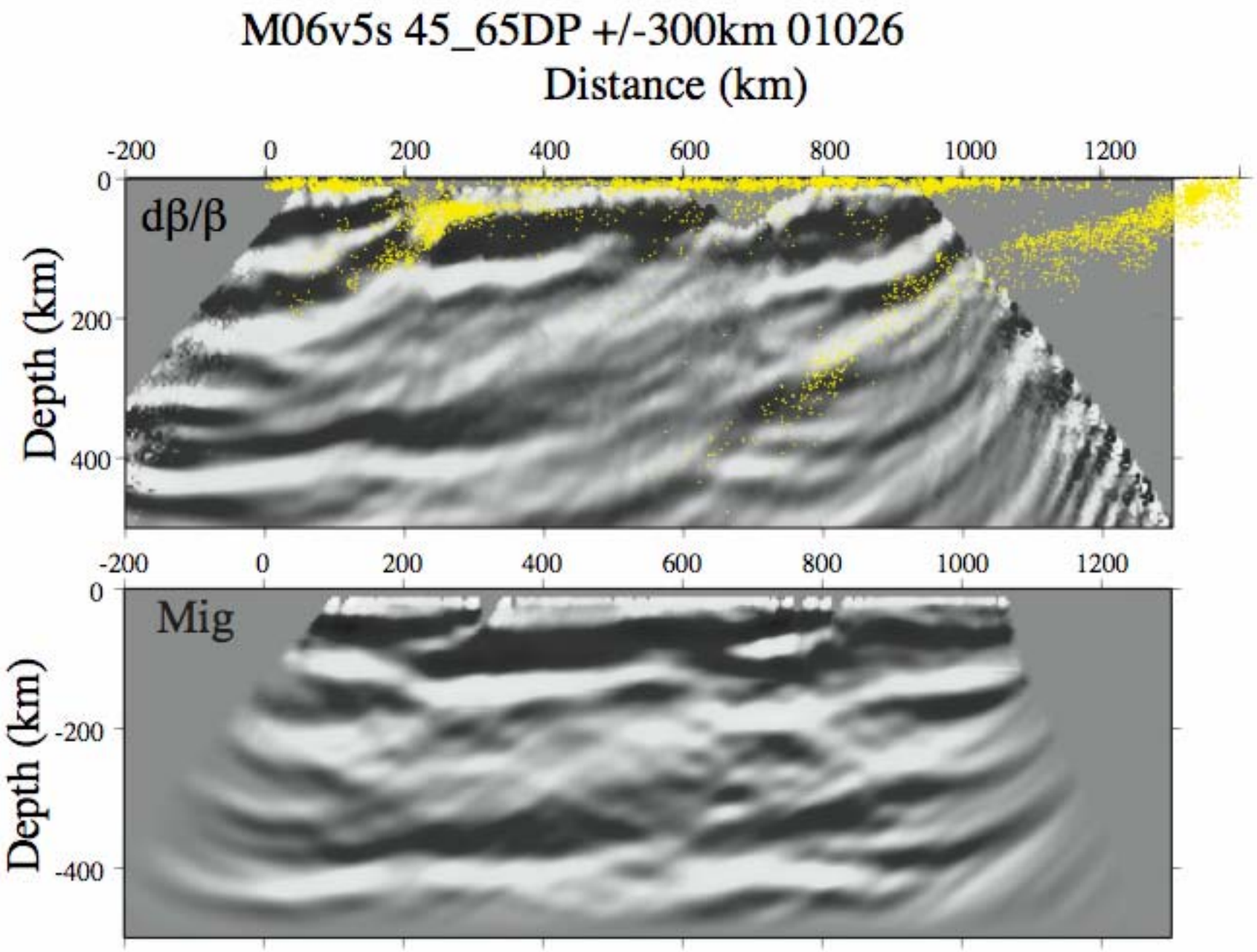
M06v5s 45_65DP +/-300km 01026
Distance (km)
-200
0
200
400
600
800
1000
1200
dβ/β
Depth (km)
0
200
400
Mig
-200
-400

Bostock et al.,
2001, 2002

Generalized
Radon Transform

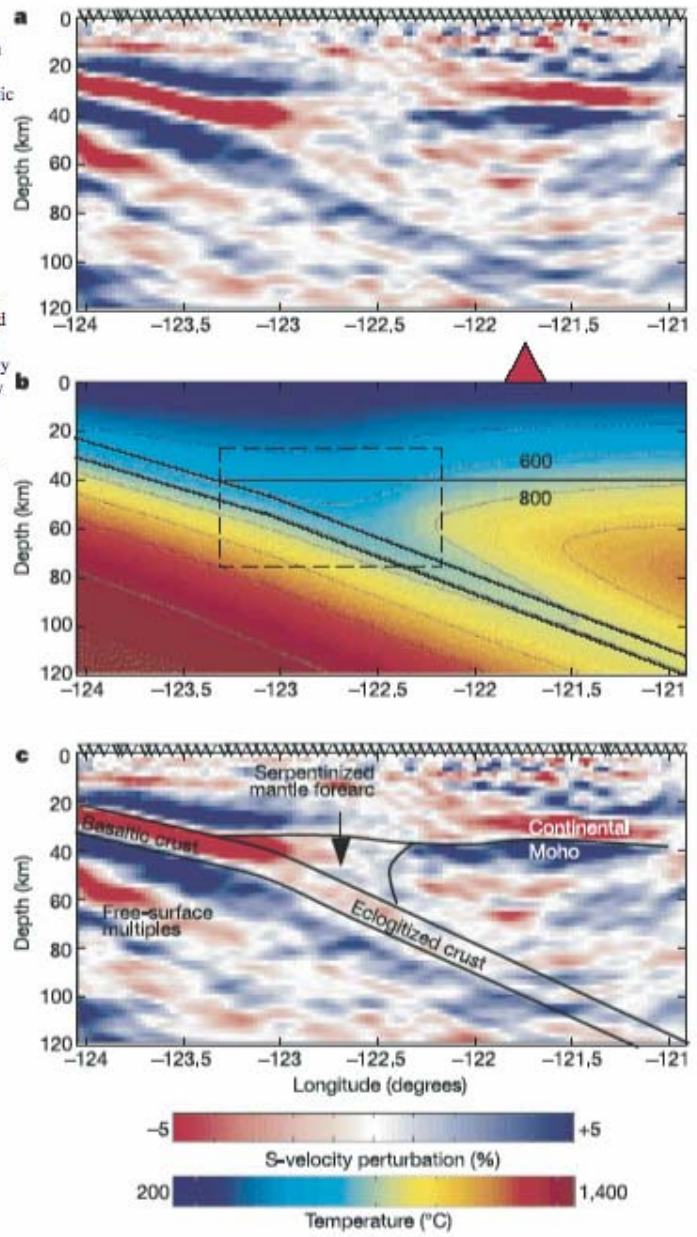

Figure 1: a) Generalized Radon Transform scattered wave image of the Cascadia subduction zone in Oregon from teleseismic data. The image shows S-wave velocity perturbation in percent from a 1-D backgroung model.

b) Cascadia subduction zone thermal structure.

c) Interpretation of S-wave velocity perturbations in light of thermal structure. The authors interpret the absent or inverted continental Moho conversion from about -123° to -122.5° as resulting from a highly serpentinized, and therefore low S velocity upper mantle, and the loss of signal from the subducting oceanic crust as due to eclogitization (from Bostock et al., 2002).